



CHORUS

This is the accepted manuscript made available via CHORUS. The article has been published as:

Multibeam Stimulated Raman Scattering in Inertial Confinement Fusion Conditions

P. Michel, L. Divol, E. L. Dewald, J. L. Milovich, M. Hohenberger, O. S. Jones, L. Berzak Hopkins, R. L. Berger, W. L. Kruer, and J. D. Moody

Phys. Rev. Lett. **115**, 055003 — Published 30 July 2015

DOI: [10.1103/PhysRevLett.115.055003](https://doi.org/10.1103/PhysRevLett.115.055003)

Multi-beam stimulated Raman scattering in ICF conditions

P. Michel,¹ L. Divol,¹ E. L. Dewald,¹ J. L. Milovich,¹ M. Hohenberger,² O. S. Jones,¹ L. Berzak Hopkins,¹ R.L. Berger,¹ W.L. Kruer,¹ and J.D. Moody¹

¹Lawrence Livermore National Laboratory, Livermore, CA 94551

²Laboratory for Laser Energetics, University of Rochester,
250 East River Road, Rochester, New York 14623-1299, USA

Stimulated Raman scattering (SRS) from multiple laser beams arranged in a cone sharing a common daughter wave is investigated for inertial confinement fusion (ICF) conditions in an inhomogeneous plasma. It is found that the shared-electron plasma wave (EPW) process, where the lasers collectively drive the same EPW, can lead to an absolute instability when the electron density reaches a matching condition dependent on the cone angle of the laser beams. This mechanism could explain recent experimental observations of hot electrons at early times in ICF experiments, at densities well below quarter-critical when two plasmon decay is not expected to occur.

Inertial Confinement Fusion (ICF) [1] experiments rely on a large number of high energy lasers to achieve controlled thermonuclear burn in the laboratory. Among several proposed approaches to ICF, two are currently most actively pursued: the indirect-drive approach [2], where the laser energy is converted into x-rays that compress a spherical DT fuel target, and the direct-drive approach [3], where the lasers directly hit and compress the target. In both schemes, laser-plasma interactions (LPI) play a crucial role, as they can lead to a degradation of the implosion performance via reduction of laser coupling to the target, drive asymmetries and fuel pre-heat via the generation of energetic electrons [4]. Recently, much attention has been given to multi-beam effects in LPI, which are relevant to experiments on ICF facilities such as the Omega laser (Rochester, NY) or the National Ignition Facility (NIF) (Livermore, CA), where many laser beams overlap in plasmas; these phenomena include crossed-beam energy transfer [5–9], two-plasmon decay (TPD) [10–13], and back- or side-scatter [14–19] (for a review of multi-beam LPI, cf. Ref. [20] and references therein).

In this Letter, we show that multiple laser beams propagating in an inhomogeneous plasma can drive a collective stimulated Raman scattering (SRS) mode in the “absolute” [21] regime at densities below quarter-critical. The process occurs when the beams, arranged in a cone geometry (as is typical of large-scale laser facilities), collectively drive an electron-plasma wave (EPW) along the cone axis near a “matching” electron density $n_{em}(\theta_v) = \cos^4(\theta_v)n_c/4$, where θ_v is the beams’ incident half-cone angle and n_c the critical density. The resulting absolute intensity threshold can be much lower than the typical overlapped intensities found in ICF experiments in the beam overlap regions. It is also orders of magnitude lower than the intensities required to achieve significant growth in the “convective” [22] regime, when $n_e < n_{em}(\theta_v)$. This instability can lead to coupling losses that ICF facilities are typically not setup to measure, as opposed to direct backscatter [23], and can also generate energetic electrons

along the cone axis — typically towards the ICF target core. Recent observations of hot electrons in NIF experiments at densities well below quarter-critical, when TPD is not expected to occur, are shown to be consistent with the collective SRS instability.

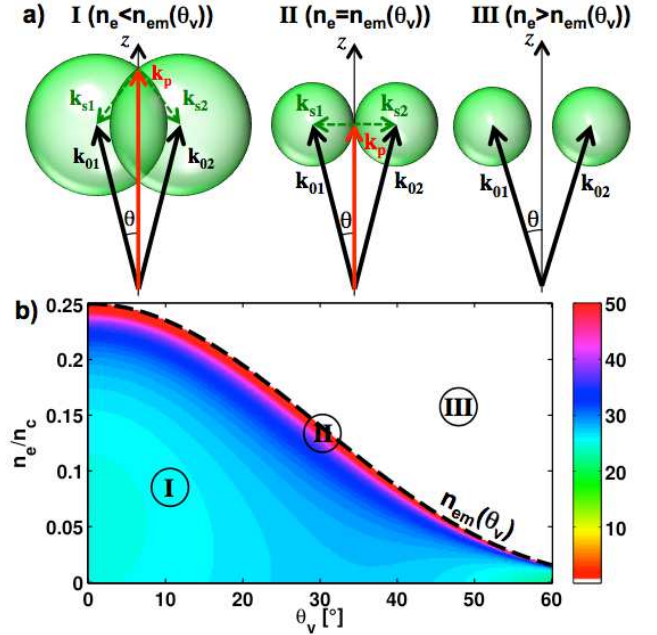


FIG. 1. a) Geometry of collective SRS via a shared-EPW: the instability is convective for $n_e < n_{em}(\theta_v)$ (I), absolute for $n_e = n_{em}(\theta_v)$ (II), and cannot exist for $n_e > n_{em}(\theta_v)$ (III). b) Convective gain vs. n_e and θ_v , for an overlapped intensity of 10^{16} W/cm² (with polarization smoothing) and $L_n=1$ mm.

The interaction geometry is represented in Fig. 1(a). N laser beams arranged in a cone with axis direction z propagate in a plasma with an electron density gradient along z and a local scale length $L_n = n_e(z)/[dn_e(z)/dz]$. In the remainder of the paper, θ will denote the half-cone angle *in the plasma*, related to the incident angle in vacuum θ_v via Snell’s law, $\sin[\theta(z)] = \sin(\theta_v)[1 - n_e(z)/n_c]^{-1/2}$ where n_c is the critical electron density

for the laser wavelength λ_0 . The N lasers beams' vector potentials $\hat{\mathbf{a}}_{0j} = \text{Re}[\mathbf{a}_{0j}\exp(i\psi_{0j})]$ (with $1 \leq j \leq N$ and $\psi_{0j} = \mathbf{k}_{0j} \cdot \mathbf{r} - \omega_0 t$, where \mathbf{k}_{0j} and ω_0 are the beam's wave-number and frequency) are normalized to e/mc^2 , so that $|a_{0j}| = 0.855 \times 10^{-2} \sqrt{I_{14} \lambda_{0\mu}^2}$ where I_{14} is the laser intensity in units of 10^{14} W/cm² and $\lambda_{0\mu}$ the laser wavelength in microns. The lasers are coupled to N scattered electromagnetic waves ($\hat{\mathbf{a}}_{sj} = \text{Re}[\mathbf{a}_{sj}\exp(i\psi_{sj})]$ with $\psi_{sj} = \mathbf{k}_{sj} \cdot \mathbf{r} - \omega_s t$) via a shared EPW, whose density modulation $\delta\hat{n} = \text{Re}[\delta n \exp(i\psi_p)]$ is phase-matched to each pair of laser and SRS wave: $\forall j : \psi_p = \psi_{0j} - \psi_{sj}$. For a given laser beam, the possible scattered light wavevectors define a sphere of radius $k_{sj}(z) = (\omega_0/c)[1 - 2\sqrt{n_e(z)/n_c}]^{1/2}$ around \mathbf{k}_{0j} [cf. Fig. 1(a)]. Therefore, the N beams can only share a common EPW if all the spheres intersect, i.e. if $k_s \geq k_0 \sin(\theta)$, or equivalently, if:

$$n_e \leq n_{em}(\theta_v) \equiv \frac{n_c}{4} \cos^4(\theta_v), \quad (1)$$

which is represented as the dashed curve in Fig. 1(b). Below that density, intersection between all N spheres occurs at two points [24], defining two possible shared EPWs. The coupling can be described starting from the wave equations for the scattered SRS waves and the shared-EPW in the fluid limit: $(\partial_t^2 - c^2 \nabla^2 + \omega_{pe}^2) \hat{\mathbf{a}}_{sj} = -\omega_{pe}^2 \hat{\mathbf{a}}_{0j} \delta\hat{n}/n_e$ and $(\partial_t^2 - 3v_e^2 \nabla^2 + \omega_{pe}^2) \delta\hat{n}/n_e = c^2 \nabla^2 (\sum_j \hat{\mathbf{a}}_{sj} \cdot \hat{\mathbf{a}}_{0j})$, where ω_{pe} and v_e are the plasma frequency and electron thermal velocity; phase-mismatched terms ($\psi_{0j} - \psi_{sj} - \psi_p \neq 0$) are negligible as long as the SRS instability doesn't grow faster than the SRS frequency [14]. Fourier-analyzing these coupled equations assuming a uniform plasma and plane laser waves gives the multi-beam SRS growth rate: $\gamma^2 = (k_p^2 c^2 \omega_{pe} / 16 \omega_s) \sum_j |a_{0j}|^2 \cos^2(\phi_j)$, where k_p is the shared EPW's wave-vector amplitude and $\cos(\phi_j) = \mathbf{a}_{0j} \cdot \mathbf{a}_{sj} / |a_{0j}| |a_{sj}|$. The growth rate expression is similar to the single-beam case except for the substitution $|a_0|^2 \rightarrow \sum_j |a_{0j}|^2 \cos^2(\phi_j)$ [4]. The EPW with the largest wave-vector k_p , which is the one represented in Fig. 1(a)-I, has the highest SRS growth rate.

For a linear density gradient along z , the well-known Rosenbluth convective gain formula [25] provides the spatial (intensity) amplification gain of an electromagnetic perturbation propagating through a resonance region where $\kappa(z) \equiv k_{0z}(z) - k_{sz}(z) - k_{pz}(z)$ goes through zero: $G = 2\pi\gamma^2 / (V_{sz} V_{pz} d\kappa/dz)$, where V_{sz} , V_{pz} are the z -components of the scattered and plasma wave group velocities, respectively, and $V_{pz} d\kappa/dz \approx -V_{pz} dk_{pz}/dz \approx \omega_{pe}/2L_n$. In the shared-EPW geometry considered here and with the aforementioned multi-beam SRS growth rate γ , we get:

$$G = \frac{\pi L_n \sum_j |a_{0j}|^2 \cos^2(\phi_j) \frac{k_p^2}{k_{sz}}}{4}, \quad (2)$$

where k_p and $k_{sz} (\equiv \mathbf{k}_s \cdot \mathbf{z})$ are given by $k_p = k_0 \cos(\theta) + \sqrt{k_s^2 - k_0^2 \sin^2(\theta)}$, $k_{sz} = k_s^2 - k_0^2 \sin^2(\theta)$. With polarization smoothing (P.S.), the energy of a beam (or a NIF "quadruplet", which will be treated as a beam with P.S. in the following) is equally distributed between an azimuthal and a radial polarization components with $\cos^2(\phi_j) = 1$ and $\cos^2(\phi_j) = \sin^2(\theta)$, respectively: $\cos^2(\phi_j)$ can thus be replaced by $[1 + \sin^2(\theta)]/2$.

The convective gain with P.S. is shown in Fig. 1(b). For the chosen laser and plasma parameters, $L_n=1$ mm and 10^{16} W/cm² overlapped intensity, the gain is ~ 25 -30 for densities below $n_{em}(\theta_v)$. Note that the convective gain formula [Eq. (2)] can also be applied to the situation of multi-beam SRS via a shared-electromagnetic wave (EMW) (in the same geometry as studied by Dubois for homogeneous plasmas [14]); however we find that the convective gain for the collective shared-EMW instability is systematically smaller than for the convective shared-EPW by about a factor two, mainly because the polarization of the shared-EMW cannot be aligned with more than two (azimuthally opposed) laser beams.

As n_e approaches n_{em} , the SRS light scattered off the shared-EPW propagates nearly perpendicular to the density gradient [cf. Fig. 1(a)-II], and can thus remain resonant until it refracts towards lower density regions. The Rosenbluth analysis is then invalid (G diverges for $k_{sz} = 0$), and the instability can become absolute [26, 27]. The single-beam situation was comprehensively described by Afeyan and Williams for arbitrary incidence angles [28]; Fourier-analyzing the coupled EMW and EPW wave equations in the presence of a linear density gradient leads to a Schrödinger equation, whose unstable localized solutions give the threshold for absolute instability (Eq. (48) of Ref. [28]) (that analysis closely followed the one used by Simon for TPD [29]). With our notations, that threshold reads:

$$|a_0|^2 \cos^2(\phi) > \frac{(n_e/n_c)^{1/3}}{(k_p/k_0)^2 (1 - n_e/n_c)} \left(\frac{c}{L_n \omega_0} \right)^{4/3}. \quad (3)$$

For a shared-EPW driven by N equal intensity-beams, the same substitution $|a_0|^2 \rightarrow \sum_j |a_{0j}|^2 \cos^2(\phi_j)$ as in the homogeneous case is still valid. Since the absolute instability occurs at $n_e = n_{em}(\theta_v)$ [Eq. (1)], where $k_p = k_0 \cos(\theta)$, re-inserting into Eq. 3 gives the N beam-absolute threshold with a shared EPW, which now depends only on L_n and θ_v :

$$N |a_{0j}|^2 > f^{-1}(\theta_v) \left(\frac{\pi L_n}{\lambda_0} \right)^{-4/3}, \quad (4)$$

where the geometrical function f is given by: $f(\theta_v) = [4 \cos^{2/3}(\theta_v) - \cos^{8/3}(\theta_v)] \cos^2[\phi(\theta_v)]$. With P.S. ($\cos^2(\phi) = [1 + \sin^2(\theta)]/2$), we have $f(\theta_v) \approx 2 \pm 0.2$ for any θ_v between 20° and 60°: the threshold then only

depends on L_n , and can be expressed (within $\pm 10\%$) in the simpler form and in practical units as follows:

$$I_{14}\lambda_{0\mu}^2 \geq 1.5 \times 10^3 (L_n/\lambda_0)^{-4/3}, \quad (5)$$

where I_{14} is the overlapped intensity in units of 10^{14} W/cm².

The absolute intensity threshold for $L_n=1$ mm and 351 nm light is in the mid- 10^{13} W/cm², i.e. more than two orders of magnitudes below the overlapped intensity required to get significant gain for the convective mode at $n_e < n_{em}(\theta_v)$, per Fig. 1(b). Thus the absolute shared-EPW mode is expected to be the dominant multi-beam SRS mechanism, as long as the matching density $n_{em}(\theta_v)$ is present. The geometry and density matching conditions also lead to $(k_p\lambda_D)^2 = [4\cos^{-2}(\theta_v) - 1]T_e/m_e c^2$, where λ_D is the Debye length and T_e the electron temperature; therefore, Landau damping only becomes significant ($k_p\lambda_D \geq 0.3$) for large cone angles ($\theta_v \geq 50^\circ$) and at temperatures above 5 keV, and is thus not expected to impede the multi-beam SRS instability for most ICF conditions.

Next we compare the threshold for the collective shared-EPW instability to the single-beam side-scatter SRS threshold. The single-beam mode's geometry maximizes k_p while satisfying $\mathbf{k}_s \cdot \nabla n_e = 0$ and the alignment of the polarization vectors of the laser beam and its scattered light wave ($\cos(\phi_j) = 1$) [28], as shown in Fig. 2(a). The single-beam absolute threshold when the laser polarization is along the radial (θ) or azimuthal (ϕ) direction still follows Eq. (3), with k_p given by $k_{p\theta}^2 = k_0^2[1 + \sin^2(\theta)]$ and $k_{p\phi}^2 = k_0^2[1 + 3\sin^2(\theta)]$, respectively. One can thus write a condition on the minimum number of beams per cone required for the shared-EPW threshold to be lower than the single-beam threshold, giving the following result with P.S.:

$$N > N_{P.S.}(\theta) \equiv \frac{1 + 3\sin^2(\theta)}{\cos^2(\theta)[1 + \sin^2(\theta)]}. \quad (6)$$

If the polarization of each laser beam is purely radial, the condition becomes more stringent, leading to:

$$N > N_\theta(\theta) \equiv \frac{1 + \sin^2(\theta)}{\cos^2(\theta)\sin^2(\theta)}. \quad (7)$$

$N_{P.S.}$ and N_θ are plotted in Fig. 2(b). For most ICF facilities, the collective mode is always expected to dominate when P.S. is present. However, using radial polarization instead of P.S. would impose nonalignment of the polarizations of the lasers and their SRS waves [$\cos(\phi_j) = \sin(\theta)$], which would both increase the absolute threshold [via $f(\theta_v)$ in Eq. (4)] and help prevent the collective mode from dominating over the single-beam modes, especially at small angles.

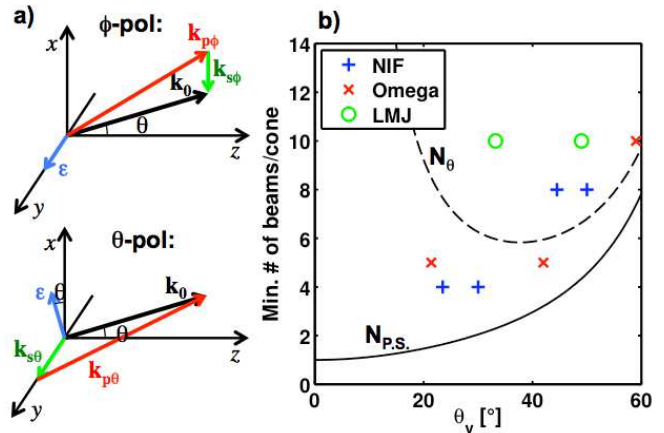


FIG. 2. a) Geometry of the dominant SRS side-scatter mode for a single laser beam, azimuthally (ϕ) or radially (θ) polarized; ϵ is the direction of both the laser beam and its scatter light wave's polarizations. b) $N_{P.S.}$ and N_θ [from Eqs (6),(7)] as a function of θ_v : the collective shared-EPW instability dominates over each individual laser beam's SRS side-scatter when the number of beams per cone N is larger than $N_{P.S.}$ with P.S. or N_θ with radial polarization. Also shown are typical number of beams per cone on the NIF, Omega and Laser Megajoule (LMJ, France) facilities.

The absolute shared-EPW process has distinctive experimental signatures, due to the unique relation between the cone angle and the electron density where it occurs. Fig. 3 shows three observables that could be measured in experiments: i) the scattered light wavelength λ_s , given by $\omega_s(\theta_v) \simeq \omega_0 - \omega_{pm}(\theta_v) = \omega_0[1 - \cos^2(\theta_v)/2]$ (where $\omega_{pm} = \omega_0\sqrt{n_{em}(\theta_v)/n_c}$); ii) the temperature of the suprathermal electrons accelerated by the EPW near its phase velocity $v_p = \omega_{pm}/k_p$, $T_{hot} \simeq \frac{1}{2}mv_p^2 = mc^2 \cos^2(\theta_v)/[8 - 2\cos^2(\theta_v)]$; and iii) the scattered light's exit angle θ_s , estimated after its refraction away from the turning point where it originates: $\cos^2(\theta_s) = \omega_{pm}^2(\theta_v)/\omega_s^2(\theta_v)$ [4]. T_{hot} is significantly higher than for backscatter SRS [9, 30], due to the smaller k_p associated with the absolute shared-EPW geometry.

Finally, we discuss experimental results at the NIF where the observation of hot electrons is consistent with absolute multi-beam SRS. In these experiments, only the first two nanoseconds of an ICF laser pulse (the ‘‘picket’’) were used [31]. The role of the picket in indirect-drive is to blow down the window at the laser entrance holes (LEH) of the cylindrical cavity (the ‘‘hohlraum’’), and to launch a first shock onto the fuel pellet. The nuclear fuel is highly sensitive to preheat from hot electrons at these early times; the mitigation technique against TPD (usually the primary source of hot electrons in the picket) consists in blowing the window with only two cones of beams (the ‘‘inner beams’’, at $\theta_v = 23.5^\circ$ and 30°) at low intensity (below the TPD threshold), and a few hundreds of picoseconds later, after the window density has dropped

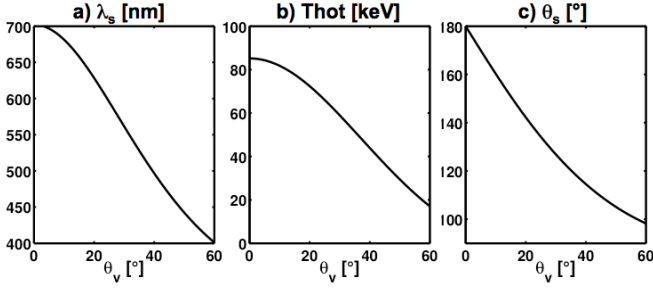


FIG. 3. Experimental signatures of shared-EPW SRS vs. incident cone angle: a) scattered light wavelength λ_s ; b) hot electron temperature $T_{hot} = \frac{1}{2}m(\omega_{pm}/k_p)^2$; c) scattered light exit angle in vacuum (with respect to z , i.e. 180° is pure backscatter).

below quarter-critical (eliminating the risk of TPD [30]), firing the remaining “outer” cones ($\theta_v=44.5^\circ$ and 50°) at higher power to launch the first shock. This is illustrated in Fig. 4(a), which shows the laser pulse for the two NIF shots investigated here.

The two shots we are comparing were nearly identical except for their hohlraum gas-fill density: 0.6 mg/cc in one case, vs. a “near-vacuum hohlraum” (NVH) at 0.03 mg/cc in the other. Density profiles at the LEH from hydrodynamics simulations are shown in Fig. 4(b)–(d) at $t_1=0.2$, $t_2=0.5$ and $t_3=1$ ns. The density was averaged over a 1.2 mm diameter region at the LEH, corresponding to the laser beams’ overlap area (radial density variations over that region were very small). The time-resolved FFLEX diagnostic [32, 33] recorded a short burst (≤ 250 ps) of hot electrons at t_2 in the 0.6 mg/cc shot only, with a temperature $T_{hot} = 42 \pm 3$ keV and energy $E_{hot} = 13 \pm 3$ J. The NVH shot on the other hand detected no hot electrons at all.

The observation of hot electrons in the 0.6 mg/cc shot only is consistent with absolute multi-beam SRS. First, we note that the inner beams are never at risk: at t_1 , when they reach their peak power and the density is still at $n_{em}(30^\circ)=0.14n_c$ within the overlap region (for the 0.6 mg/cc shot only), the density gradient is too steep ($L_n \approx 150 \mu\text{m}$) and the overlapped intensity too low (1.4×10^{14} W/cm²) to reach the absolute threshold of 3.8×10^{14} W/cm² per Eq. (5). On the other hand, for the outer beams, the density matches $n_{em}(50^\circ)=4.3\%n_c$ (0.6 mg/cc shot only) until t_3 , after which the density bump both drops below $n_{em}(50^\circ)$ and exits the 50° overlap region [dashed black box from $z=5.5$ to 6.2 mm in Fig. 4(d)]. Between t_2 and t_3 , the overlapped 50° cone intensity is 1.5×10^{15} W/cm² [Fig. 4(a)], forty times above the absolute threshold for shared-EPW SRS, $I_{thr} = 3.8 \times 10^{13}$ W/cm² (with $L_n \approx 900 \mu\text{m}$). This is consistent with the observation of hot electrons at that time for the 0.6 mg/cc shot only. The absence of hot electrons in the couple hundreds ps preceding t_3 in the experiment (despite

being above threshold) might be due to differences in the density drop between the model and the experiment. For the NVH, the window density drops fast enough (due to the absence or counter-pressure from the hohlraum gas-fill) to stay out of the absolute SRS matching density ($n_e < n_{em}$) while the outer beams are on.

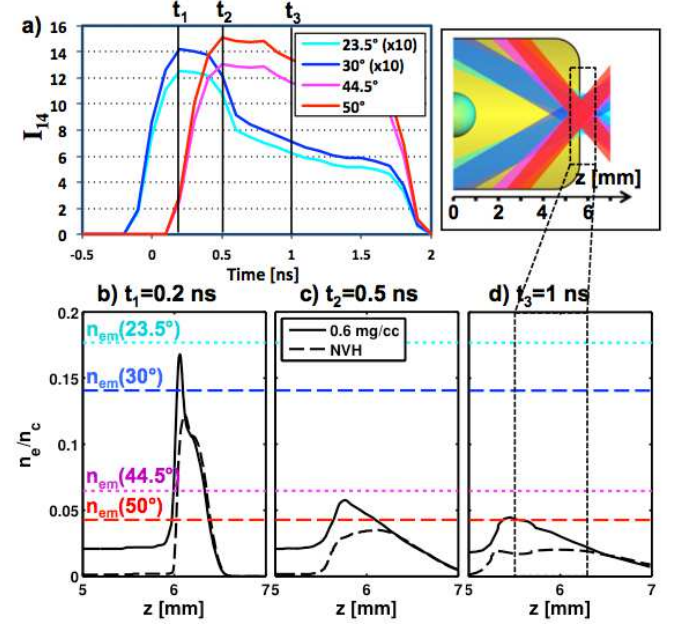


FIG. 4. a) Overlapped intensities in units of 10^{14} W/cm² for the four NIF cones of beams, at 23.5° , 30° , 44.5° and 50° ($\times 10$ for the 23.5° and 30°), and beams overlap geometry (insert). b)–d) Simulated n_e/n_c vs. z (hohlraum axis) at the LEH for two NIF shots with hohlraum gas-fill of 0.6 mg/cc and 0.03 mg/cc (“near-vacuum hohlraum”, NVH) at $t_1=0.2$ ns, $t_2=0.5$ ns and $t_3=1$ ns. Also shown are the matching densities $n_{em}(\theta_v)$ [Eq. (1)] for the four cone angles. The 50° cone is forty times above threshold at $n_{em}(50^\circ)$ between t_2 and t_3 for the 0.6 mg/cc shot only (after t_3 , the density bump has both dropped below $n_{em}(50^\circ)$ and moved out of the 50° cone overlap region, shown as a dashed black box between $z=5.5$ and 6.2 mm: multi-beam SRS is thus expected to stop). The density in the NVH drops fast enough to stay below n_{em} , eliminating the risk of absolute multi-beam SRS. This is consistent with the observation of hot electrons on the 0.6 mg/cc shot only, at time t_2 for a duration ≤ 250 ps.

In summary, we have shown that multiple laser beams propagating in a inhomogeneous plasma can drive an absolute collective SRS instability via a shared-EPW along the beams’ cone axis, when the electron density matches the resonance condition for a given cone angle θ_v , $n_{em} = \cos^4(\theta_v)n_c/4$. This process could lead to unmeasured scattering losses and generation of hot electrons along the cone axis. The collective shared-EPW mode dominates over the single-beam SRS side-scatter modes when a minimum number of beams per cone is present; that condition is satisfied for most ICF facilities. Hot electrons signatures (absent quarter-critical

densities) have been identified in recent NIF experiments that are consistent with the collective SRS instability. This study suggests several mitigation strategies, such as electron density tuning (to avoid densities near $n_{em}(\theta_v)$ in the beams overlap region), or by lowering the overlapped intensity, or by adjusting the beams' polarization arrangement.

This work was performed under the auspices of the U.S. Department of Energy by Lawrence Livermore National Laboratory under Contract DE-AC52-07NA27344.

-
- [1] J. Nuckolls and L. Wood, *Nature* **239**, 139 (1972).
- [2] J. Lindl, *Phys. Plasmas* **2**, 3933 (1995).
- [3] R. McCrory, J. Soures, C. Verdon, F. Marshall, S. Letzring, S. Skupsky, T. Kessler, R. Kremens, J. Knauer, H. Kim, *et al.*, *Nature* **335**, 225 (1988).
- [4] W. L. Kruer, *The physics of laser plasma interactions* (Westview Press, 2003).
- [5] W. L. Kruer, S. C. Wilks, B. B. Afeyan, and R. K. Kirkwood, *Phys. Plasmas* **3**, 382 (1996).
- [6] I. V. Igumenshchev, W. Seka, D. H. Edgell, D. T. Michel, D. H. Froula, V. N. Goncharov, R. S. Craxton, L. Divol, R. Epstein, R. Follett, J. H. Kelly, T. Z. Kosc, A. V. Maximov, R. L. McCrory, D. D. Meyerhofer, P. Michel, J. F. Myatt, T. C. Sangster, A. Shvydky, S. Skupsky, and C. Stoeckl, *Phys. Plasmas* **19**, 056314 (2012).
- [7] D. H. Froula, I. V. Igumenshchev, D. T. Michel, D. H. Edgell, R. Follett, V. Y. Glebov, V. N. Goncharov, J. Kwiatkowski, F. J. Marshall, P. B. Radha, W. Seka, C. Sorce, S. Stagnitto, C. Stoeckl, and T. C. Sangster, *Phys. Rev. Lett.* **108**, 125003 (2012).
- [8] P. Michel, L. Divol, E. A. Williams, S. Weber, C. A. Thomas, D. A. Callahan, S. W. Haan, J. D. Salmonson, S. Dixit, D. E. Hinkel, M. J. Edwards, B. J. MacGowan, J. D. Lindl, S. H. Glenzer, and L. J. Suter, *Phys. Rev. Lett.* **102**, 025004 (2009).
- [9] P. Michel, L. Divol, R. P. J. Town, M. D. Rosen, D. A. Callahan, N. B. Meezan, M. B. Schneider, G. A. Kyrala, J. D. Moody, E. L. Dewald, K. Widmann, E. Bond, J. L. Kline, C. A. Thomas, S. Dixit, E. A. Williams, D. E. Hinkel, R. L. Berger, O. L. Landen, M. J. Edwards, B. J. MacGowan, J. D. Lindl, C. Haynam, L. J. Suter, S. H. Glenzer, and E. Moses, *Phys. Rev. E* **83**, 046409 (2011).
- [10] C. Stoeckl, R. E. Bahr, B. Yaakobi, W. Seka, S. P. Regan, R. S. Craxton, J. A. Delettrez, R. W. Short, J. Myatt, A. V. Maximov, and H. Baldis, *Phys. Rev. Lett.* **90**, 235002 (2003).
- [11] R. W. Short, *Bull. Am. Phys. Soc.* **55** (2010).
- [12] D. T. Michel, A. V. Maximov, R. W. Short, S. X. Hu, J. F. Myatt, W. Seka, A. A. Solodov, B. Yaakobi, and D. H. Froula, *Phys. Rev. Lett.* **109**, 155007 (2012).
- [13] J. Zhang, J. F. Myatt, R. W. Short, A. V. Maximov, H. X. Vu, D. F. DuBois, and D. A. Russell, *Phys. Rev. Lett.* **113**, 105001 (2014).
- [14] D. F. DuBois, B. Bezzerides, and H. A. Rose, *Phys. Fluids B* **4**, 241 (1992).
- [15] W. Kruer, *Bull. Am. Phys. Soc.* **52** (2007).
- [16] C. Labaune, H. A. Baldis, E. Schifano, B. S. Bauer, A. Maximov, I. Ourdev, W. Rozmus, and D. Pesme, *Phys. Rev. Lett.* **85**, 1658 (2000).
- [17] W. Seka, H. A. Baldis, J. Fuchs, S. P. Regan, D. D. Meyerhofer, C. Stoeckl, B. Yaakobi, R. S. Craxton, and R. W. Short, *Phys. Rev. Lett.* **89**, 175002 (2002).
- [18] R. K. Kirkwood, P. Michel, R. London, J. D. Moody, E. Dewald, L. Yin, J. Kline, D. Hinkel, D. Callahan, N. Meezan, E. Williams, L. Divol, B. L. Albright, K. J. Bowers, E. Bond, H. Rose, Y. Ping, T. L. Wang, C. Joshi, W. Seka, N. J. Fisch, D. Turnbull, S. Suckewer, J. S. Wurtele, S. Glenzer, L. Suter, C. Haynam, O. Landen, and B. J. MacGowan, *Phys. Plasmas* **18**, 056311 (2011).
- [19] D. Turnbull, P. Michel, J. Ralph, L. Divol, J. Ross, L. Berzak Hopkins, A. Kritcher, D. Hinkel, and J. Moody, *Phys. Rev. Lett.* **114**, 125001 (2015).
- [20] J. F. Myatt, J. Zhang, R. W. Short, A. V. Maximov, W. Seka, D. H. Froula, D. H. Edgell, D. T. Michel, I. V. Igumenshchev, D. E. Hinkel, P. Michel, and J. D. Moody, *Phys. Plasmas* **21**, 055501 (2014).
- [21] "Absolute" instability: a spatially localized disturbance grows exponentially in time.
- [22] "Convective" instability: the disturbances undergo finite spatial amplification while propagating through a resonance region.
- [23] J. D. Moody, P. Datte, K. Krauter, E. Bond, P. A. Michel, S. H. Glenzer, L. Divol, C. Niemann, L. Suter, N. Meezan, B. J. MacGowan, R. Hibbard, R. London, J. Kilkenny, R. Wallace, J. L. Kline, J. Jackson, K. Knittel, G. Frieders, B. Golick, G. Ross, K. Widmann, J. Jackson, S. Vernon, and T. Clancy, *Rev. Sci. Instrum.* **81**, 10D921 (2010).
- [24] For $N=2$ beams only, the intersection between two k_s spheres defines a circle, i.e. an infinity of shared-EPWs; however for $N \geq 3$, which is the most relevant situation for all ICF facilities, one can easily verify that the intersection between all N spheres occurs only at two points located on the cone angle.
- [25] M. N. Rosenbluth, *Phys. Rev. Lett.* **29**, 565 (1972).
- [26] C. S. Liu, M. N. Rosenbluth, and R. B. White, *Phys. Rev. Lett.* **31**, 697 (1973).
- [27] C. S. Liu, M. N. Rosenbluth, and R. B. White, *Phys. Fluids* **17**, 1211 (1974).
- [28] B. B. Afeyan and E. A. Williams, *Phys. Fluids* **28**, 3397 (1985).
- [29] A. Simon, R. W. Short, E. A. Williams, and T. Dewandre, *Phys. Fluids* **26**, 3107 (1983).
- [30] S. P. Regan, N. B. Meezan, L. J. Suter, D. J. Strozzi, W. L. Kruer, D. Meeker, S. H. Glenzer, W. Seka, C. Stoeckl, V. Y. Glebov, T. C. Sangster, D. D. Meyerhofer, R. L. McCrory, E. A. Williams, O. S. Jones, D. A. Callahan, M. D. Rosen, O. L. Landen, C. Sorce, and B. J. MacGowan, *Phys. Plasmas* **17**, 020703 (2010).
- [31] E. L. Dewald, J. L. Milovich, P. Michel, O. L. Landen, J. L. Kline, S. Glenn, O. Jones, D. H. Kalantar, A. Pak, H. F. Robey, G. A. Kyrala, L. Divol, L. R. Benedetti, J. Holder, K. Widmann, A. Moore, M. B. Schneider, T. Döppner, R. Tommasini, D. K. Bradley, P. Bell, B. Ehrlich, C. A. Thomas, M. Shaw, C. Widmayer, D. A. Callahan, N. B. Meezan, R. P. J. Town, A. Hamza, B. Dzenitis, A. Nikroo, K. Moreno, B. Van Wousterghem, A. J. Mackinnon, S. H. Glenzer, B. J. MacGowan, J. D. Kilkenny, M. J. Edwards, L. J. Atherton, and E. I. Moses, *Phys. Rev. Lett.* **111**, 235001 (2013).
- [32] E. L. Dewald, C. Thomas, S. Hunter, L. Divol, N. Meezan, S. H. Glenzer, L. J. Suter, E. Bond, J. L. Kline, J. Celeste,

- D. Bradley, P. Bell, R. L. Kauffman, J. Kilkenny, and O. Landen, *Rev. Sci. Instrum.* (2010).
- [33] M. Hohenberger, F. Albert, N. E. Palmer, J. J. Lee, T. Döppner, L. Divol, E. L. Dewald, B. Bachmann, A. G. MacPhee, G. LaCaille, D. K. Bradley, and C. Stoeckl, *Rev. Sci. Instrum.* **85**, 11D501 (2014).